Investigation of Characteristics in Mountain Area with the Aim of Collecting Data for Modelling Flow Turbulent Parameters in a Wind Farm Located in a Coastal Area

Sergei Strijhak [a], Konstantin Koshelev [b] and Arina Kryuchkova [c]
Ivannikov Institute for System Programming of the RAS, 25 Alexander Solzhenitsyn Street, 109004, Moscow, Russia

Keywords: Wind Energy, Wind Farm, Crete, Russia, Complex Terrain, Mountain, Large-Eddy Simulation, Finite Volume Method, Mesh, SOWFA Library, Solver, Wind Turbines, Velocity, Pressure, Temperature, Computer Nodes.

Abstract: The article summarize results of the study of wind farms located on the island of Crete and in Russia using different solvers of open source SOWFA library. Applying large-eddy simulation approach allows to take into account the orography of the area, different physical processes like lower-level jets and will assess the impact of the wind farm and turbulent wakes on the local microclimate of the region.

1 INTRODUCTION

Wind energy is an important part of renewable energy sources in many countries. In the last decades the flow simulation for wind farms and turbines have been studied more because it is a very good alternative for producing energy. The turbulent wakes dynamics and wind turbines performance in wind farms are the questions of the great interest now for the scientific community. Large-eddy simulation (LES) has recently been well applied in the context of numerical simulation of a flow over wind turbines on flat and complex terrains (Mehta et al., 2014; Stevens and Meneveau, 2017). The region of the island of Crete encourages siting of wind farms due to the strong wind potential and insular rough terrain (Tsoutsos et al., 2015; Kanellopoulos et al., 2013).

In this work a procedure for collecting data in mountain area for modelling flow turbulent parameters in wind farm is described, numerical simulation of new wind farm in Ulyanovsk oblast of Russian Federation (RF) was also carried out using open source SOWFA library. The paper is organized as follows. In section 2 we provide information about a wind farm on the island of Crete, its geographical location, surface topography and meteo data in this region. We describe the SOWFA library and mathematical model to handle the problem of creating numerical case including domain and mesh settings. In Section 3 we give information about a new wind farm in Russia, its geographical location and meteo data. The details of the geometrical setup, computational mesh as well as boundary and initial conditions are provided there. Some results on numerical simulation of wind farm with 14 wind turbines are presented. The main conclusions are presented in Section 4.

2 WIND FARM ON CRETE WITH COMPLEX TERRAIN

A rather large wind farm is located in a mountainous area on the island of Crete, near the village of Xirolimni (Figure 1,2). The wind farm has geographic coordinates from N35 10 '12 "E26 08' to N35 07' 48 "E26 14'. The wind farm was located on different levels on mountain terrain and has different models of Horizontal Axis Wind Turbine (HAWT) with Power from 0.3 MW till 0.8 MW (Figure 3,4). Due to the fact that the wind farm is located between the major coastal cities in bay area Sitia, Hagia Photia

[a] https://orcid.org/0000-0001-5525-5180
[b] https://orcid.org/0000-0002-7124-3945
[c] https://orcid.org/0000-0001-9267-8692

345

and Kato Zakros, it is necessary to assess the impact of the wind farm and turbulent wakes on the local microclimate of the region.

Figure 1: The map of the island of Crete.

The terrain orography data with the highest point of 745 meters was obtained using Google Earth Pro software from Internet and satellite imagery. The mountainous data were converted to the WGS 84 UTM 35N metric coordinate system using the QGIS open source software package. The final surface of the mountainous terrain near the village of Xirolimni was constructed using asc file format transferred to the STL format file, using in-house converter program, according to the results of the collected data on the coordinates of the complex terrain. As it was shown by measurements based on the meteorological tower data from the station, the wind was directed in this region from north-west to south-east (Kanellopoulos et al., 2013). The average wind velocity was 8.5 meters per second (Figure 5).

Figure 2: The map of the east part for the island of Crete.

Figure 3: The map of the wind farm on the island of Crete.

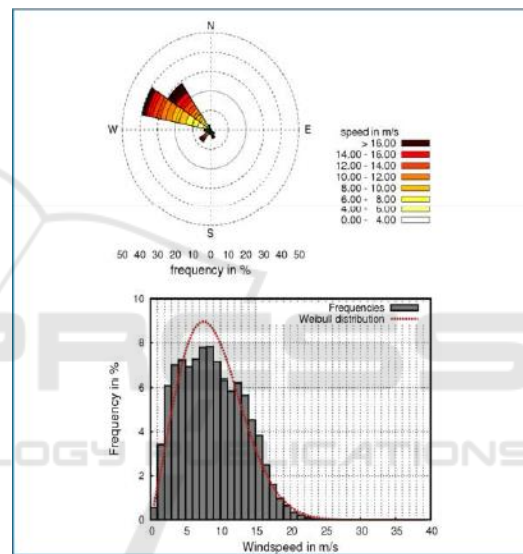Figure 4: The location of the wind turbines in the wind farm on the island of Crete.

Figure 5: The data for velocity from Meteo station.

2.1 Mathematical Model

Large-Eddy Simulation approach (LES) using finite volume method for the solution of the main equations reflecting conservation laws was used. The following equations are considered: the continuity equation (1), the momentum equation (2), the transport of scalar value - potential temperature equation (3) and other equations (4)-(8).

The sub grid-scale models are an important part of LES for Atmospheric Boundary Layer (ABL). The SGS stress tensor was raised from the filtering of the Navier-Stokes equations. The Boussinesq approximation for buoyancy force is included with the separate term in the momentum equation. The final mathematical model included the following equations (1-8).

$$\frac{\partial \bar{u}_j}{\partial x_j} = 0 \qquad (1)$$

$$\frac{\partial \bar{u}_i}{\partial t} = -\frac{\partial}{\partial x_j}\left(\bar{u}_j \bar{u}_i\right) - \frac{\partial R_{ij}^D}{\partial x_j} - \frac{\partial \tilde{p}}{\partial x_i} - \left(\frac{\partial \tilde{p}}{\partial x_i}\right)^d + \left(1 - \frac{\bar{\theta}}{\bar{\theta}^0}\right)g_i + \epsilon_{ij}f^c\bar{u}_j \qquad (2)$$

$$\frac{\partial \bar{\theta}}{\partial t} = -\frac{\partial}{\partial x_j}\left(\bar{u}_j \bar{\theta}\right) - \frac{\partial R_{\theta j}}{\partial x_j} \qquad (3)$$

$$R_{ij}^D = 2\nu^{SGS}\bar{S}_{ij} \qquad (4)$$

$$\bar{S}_{ij} = \frac{1}{2}\left(\frac{\partial \bar{u}_i}{\partial x_j} + \frac{\partial \bar{u}_j}{\partial x_i}\right) \qquad (5)$$

$$\nu^{SGS} = (C_s\Delta)^2\left(2\bar{S}_{ij}\bar{S}_{ij}\right)^{1/2} \qquad (6)$$

$$R_{\theta j} = -\frac{\nu^{SGS}}{Pr_t}\frac{\partial \bar{\theta}}{\partial x_j} \qquad (7)$$

$$\frac{\partial R_{ij}^D}{\partial x_j} = -\frac{\partial}{\partial x_j}\left(\nu^{SGS}\frac{\partial \bar{u}_i}{\partial x_j}\right) - \frac{\partial}{\partial x_j}\left[\nu^{SGS}\left(\frac{\partial \bar{u}_j}{\partial x_i} - \frac{2}{3}\frac{\partial \bar{u}_k}{\partial x_k}\delta_{ij}\right)\right] \qquad (8)$$

where, $\bar{u}_j$ is the resolved Cartesian velocity field, $\tilde{p}$ is modified pressure variable, which is the density-normalized deviation in resolved-scale static pressure from its time-averaged value (in the absence of finite time-averaged vertical gradients of temperature), $R_{ij}^D = R_{ij} - R_{kk}\delta/3$ is the deviatoric part of the sub-grid-scale (SGS) stress tensor and R_{ij} is the SGS stress tensor, R_{kk} is the trace of the stress tensor. $\left(\frac{\partial \tilde{p}}{\partial x_i}\right)^d$ is a partially constant driving pressure gradient term used to achieve a specified mean geostrophic wind, $\bar{\theta}$ is the resolved virtual potential temperature, $\bar{\theta}^0$ is the reference virtual potential temperature, g_i is the gravity vector, ϵ_{ij} - is the alternating symbol, f^c is the Coriolis parameter, and the subscripts 1, 2, and 3 refer to the x-, y-, and z-directions, respectively. $\bar{\theta}^0$ is set to the initial virtual potential temperature below the capping inversion of 300K.

All physical quantities were defined in the centre of a numerical volume cell. The features of a land topography, influence of environment stratification, Earth rotation, and change of thermal fluxes were considered for flow parameters calculation.

Large-scale vortex structures were defined by means of the filtered equations integration (Sagaut, 2010). The box filter was used for receiving the filtered equations, the small eddies which size did not exceed a step of a numerical grid were modelled by means of a Lagrangian dynamic model of Smagorinsky for subgrid turbulent viscosity - LASI (Germano et al., 1991; Meneveau et al., 1996). An additional model with restriction on dynamic Smagorinsky constant value Cs was used to avoid its negative values appearing during calculation processes.

The terms in the equations (1-8) were approximated with the first and second order of accuracy on time and space. The obtained equations for velocity, pressure, and potential temperature coupling were solved by means of an iterative algorithm PIMPLE. The procedure predictor-corrector was realized for values of velocity, pressure, and potential temperature as it was made in paper (Oliveira and Issa, 2001). The obtained system of the algebraic equations were solved by the iterative method of conjugate gradients with a preconditioner for velocity, pressure, potential temperature, stress tensor and parameters of the turbulence subgrid scale model. The total quantity of the calculated physical values (scalar, vector and tensor) depending on the selected turbulence model for subgrid scale viscosity can be from 25 to 33. In this regard the resources of High Performance Computing (HPC), or supercomputer are required.

The surface shear-stress model was calculated using Schumann model (Schumann, 1975). The stress tensor components are equal to zero on the surface, except values R13, R23.

Average and fluctuation values fields (velocity, pressure, potential temperature, sub grid viscosity, stress tensor, a thermal fluxes and others) were obtained during calculation. The ABL Solver as a part of open source library OpenFOAM 2.4 in the parallel mode was used for final modelling of parameters in turbulent flow (Churchfield et al., 2010; 2012).

2.2 Formulation of the Problem

A computational domain with dimensions of 9.4 km x 2.0 km x 4.6 km in the x-, y-, and z-directions was chosen. The STL surface of complex terrain, which was built using of Shuttle Radar Topography Mission, for the region of wind farm near the village of Xirolimni is shown in Figure 6.

The selected domain was periodic in the lateral directions; the wall conditions were applied at the lower surface; and a rigid, stress-free lid is used on the top boundary. The atmospheric stability was set to neutral with the potential temperature initialized with value of 300K along the height of 1000m above the surface. A strong capping inversion is applied in

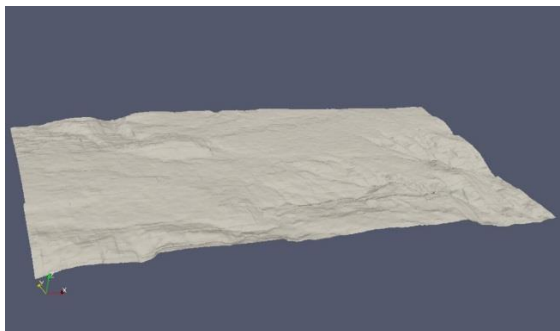which the temperature rises to 308K in the next 1000 m.

Figure 6: The STL surface for the complex terrain.

The mesh was initially created with uniform resolution using OpenFOAM blockMesh tool, and then OpenFOAM snappyHexMesh tool was used to create the 3D unstructured grid representing the real terrain. Various grids were considered with following number of cells: a) 265 200; b) 520 000; c) 2 200 000 (Figure 7).
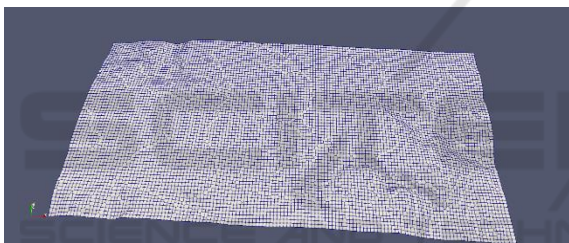

Figure 7: The mesh for the complex terrain.

The final simulation domain was defined by dimensions: 9000 meters x 4300 meters x 2000 meters in width (x-), transverse (y-), and height (z-) directions.

The simulation of the flow around mountainous terrain can be performed using the ABLSolver solver developed as a part of SOWFA open-source library. SOWFA (Simulator for On/Offshore Wind Farm Application) open-source library is based on OpenFOAM. It includes several incompressible solvers and utilities, it was developed in NREL, USA, and now is of active use by the research community (Churchfield et al., 2010; 2012). Neutral Atmospheric Boundary Layer (ABL) case with a given latitude was considered, the simulation takes place at 35º north latitude. A logarithmic velocity profile can be specified with a maximum value of 8.5 meters per second at the inlet of the computational domain. Fields of velocity, temperature, pressure, turbulent subgrid viscosity were of interest as a result of the calculation using the

Large Eddy Simulation method and dynamic Smagorinsky model for turbulent subgrid viscosity. The calculation should be done for t=20 000 seconds to take into account both night-time and day-time physical processes.

3 WIND FARM WITH FLAT TERRAIN IN RUSSIA

The wind energy industry development in Russian Federation involves designing and operation of new wind power plants and turbines. Wind farms can operate in various climatic conditions on the large territory of the country (Ulyanovsk oblast, Republic of Adygea, Taman Peninsula, Arctic region). A new wind farm was built recently in Ulyanovsk region of Russian Federation (RF) in 2017, 2018 years (Figure 8). The wind farm has geographic coordinates N54º 17 ' E48º 08'.

Similar studies were conducted for the 3D region corresponding to the ABL and the model wind farm with 2 and 12 wind turbines (Tellez-Alvarez et al., 2017, Kryuchkova et al., 2017, Strijhak et al., 2018). The ABL calculations for the area including wind farm in Ulyanovsk oblast of RF were carried out in a spatial area of 3km x 3km x 1.02km in size on numerical grids 150x150x51 and 300x300x102 during time of 20000 seconds (Tellez-Alvarez et al., 2017). The 3D numerical domain and grid are shown in Figure 9. The inlet velocity profile which is taken from field measurements is shown on Figure 10. The value of aerodynamic roughness height z0 was set to 0.1. The streamwise velocity fluctuations at 90 m above the surface for the case using numerical mesh 150 x 150 x 51 are shown in Figure 11. These fluctuations values can reach about 25% of the mean velocity value.
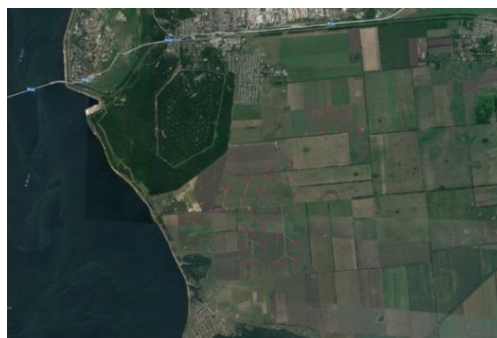

Figure 8: The territory of wind farm near the Volga River.

It is necessary to take these velocity and pressure fluctuations into account in case of physical

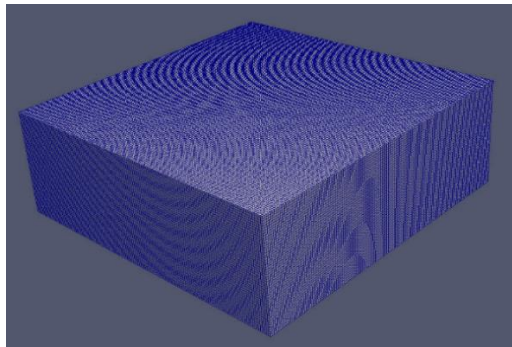parameters simulations of large wind turbines in wind farms.

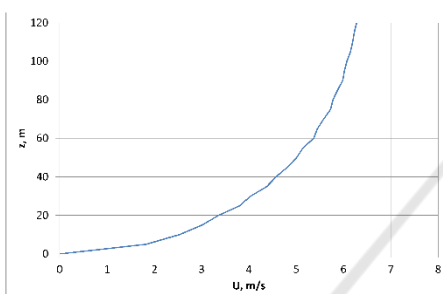Figure 9: The 3D numerical domain for ABL case.

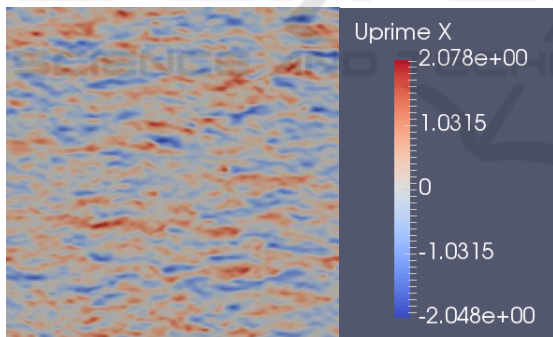
Figure 10: The inlet velocity profile for ABL case.

Figure 11: The streamwise velocity fluctuations at 90 m.

The mean potential temperature field is shown in Figure 12. Cooling ground and heating the upper layer produce internal waves dominated by the Brunt-Vaisala frequency. The obtained data from ABL simulation (Figure 11, 12) can be used for further studies of wind farms with model wind turbines of different power (Figure 13). The orography of the area can be also taken into account and the impact of the wind farm and turbulent wakes on the local microclimate of the area can be assessed.
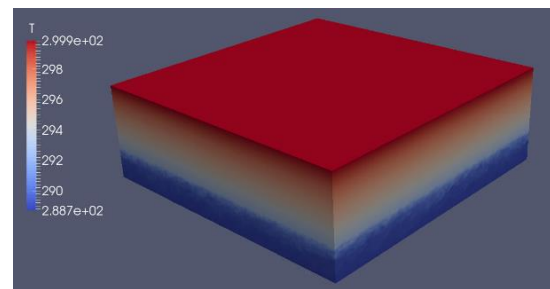

Figure 12: The temperature field for 3 D domain.

3.1 Formulation of the Problem

An additional investigation was done for the case of wind farm in Ulyanovsk oblast RF, Krasny Yar (Figure 8).
It is known that the Reynolds numbers can reach order of Re=10e7-10e8 considering the characteristic sizes of wind turbine blades. It is difficult to resolve all flow scales by means of LES since too big numerical grids would be required for this purpose.
It is well-known that Actuator Line Model (ALM) approach doesn't demand too detailed grids around the turbine blades.

Figure 13: The wind farm with 28 wind turbines.

This approach allows to represent various types of vortexes, wake, trailer, root and boundaries vortexes. In the scope of ALM turbine blades are approximated by separate flat sections with a given profile, chord, and twist. The values of lift and drag forces are collected in tables for each profile. The force projected on the flow is equal to the aerodynamic force applied on operating turbine blades. The procedure of force projection comes to a number of separate terms adding in the momentum equation. The resultant force f_i is determined with following technique:

$$f_i^{turbine}(r) = \frac{F_i^{actuator}}{eps^3 \pi^{\frac{3}{2}}} * \exp\left[\left(-\frac{r}{eps}\right)^2\right]$$

(9)

Where $F_i^{actuator}$ is actuator point force projected as a body force onto Computational Fluid Dynamics (CFD) grid, where r is the distance between CFD cell center and actuator point, eps is Gaussian filter width related to the initial intermittency. The $f_i^{turbine}(r)$ term was added as additional term in the momentum equation 2. The further details of this procedure can be found in (Sørensen and Shen, 2002). The Gauss linear Scheme was used for approximation of the convective terms, the Gauss linear corrected scheme was used for approximation of laplacian terms. To solve linear system equations the PBiCG method with DILU preconditioner was used for velocity, temperature and the GAMG method was used for pressure. The tolerance was set to 1e-6.

The first 14 wind turbines in model wind farm were considered in case with SOWFA library (Figure 13).

The diameter of rotor for wind turbine was equal to D=416 mm. The reference velocity was set to Uref=1.5 m/s. Atmospheric Boundary Layer model was introduced to represent experimental conditions. The parameters of Neutral ABL, used in our simulation, are listed in Table 1 of work (Hancock and Farr, 2014).

Each of the prototype wind turbines had 3 blades with constant cross section. The blade was made of carbon fibre with a shape of a twisted thin flat plate of 0.8 mm thickness, without using any aerofoil cross-section (Hancock and Farr, 2014). Operating tip-speed ratio (TSR) was set to 6.

The ABLSolver and pisoFoamTurbine solvers allow distinguishing the mean and turbulent wake flows behind turbines in series and the behaviour of the whole turbines array. The simulation was run in 3D box domain.

The pisoFoamTurbine solver was tested on famous Blind Test 2 with two turbines (Kryuchkova et al., 2017; Strijhak et al., 2017; Pierella et al., 2014).

The domain with following dimensions was selected: 6500 mm x 5500 mm x 1000 mm in width (x-), transverse (y-), and height (z-) directions. The data on velocity profile and wind direction were taken from the weather station and the free report of Lahmeyer International Company in Internet for the period of time from 26.05.2012 till 25.05.2013 (Figure 14-Figure 16).

The wind was directed in this area from north-west to south-east, and the average wind speed was 6.5 meters per second.

The numerical technique comprised a preliminary simulation with ABLSolver aimed to define the inlet parameters for the major domain with rotating wind turbines, the second step consisted in numerical simulations using pisoFoamTurbine.

This method is called in literature as a "Precursor" method for LES (Figure 17) (Churchfield et al., 2012).

The value of numBladePoints for the case with 14 wind turbines was set to 40, the epsilon value was set to 5.0 in Formula 9.

The resulting unstructured mesh for the test with 14 wind turbines counted 2 millions of cells.

After constructing the primary mesh with blockMesh tool the central zone with the turbines array inside was refined twice and an additional refinement was done around each turbine. The final mesh had 6 millions of cells.

The small eddies for which the size didn't exceed grid cell size were modelled by means of the Lagrangian-averaged scale-independent dynamic Smagorinsky model (Meneveau et al., 1996).
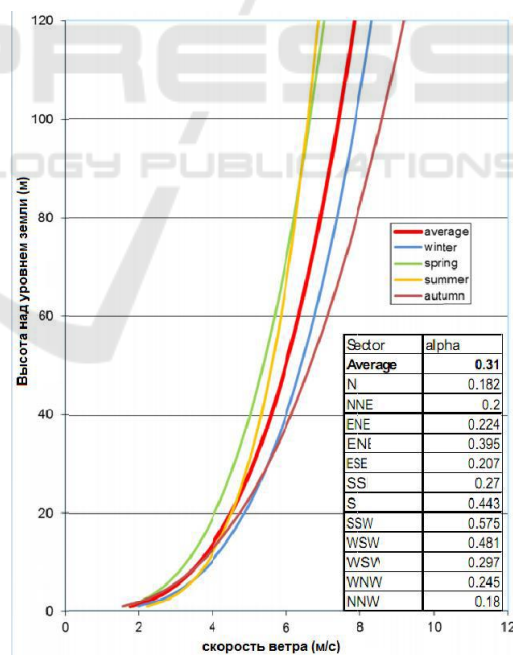

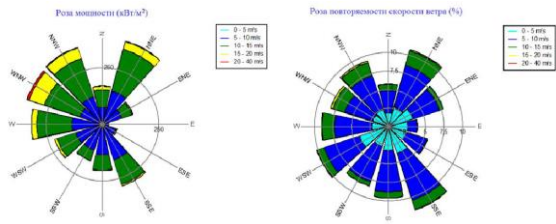Figure 14: The velocity profile in wind farm of Ulyanovsk oblast of RF.

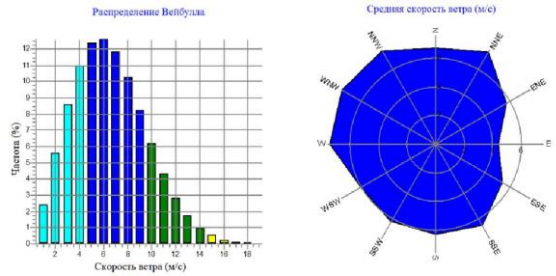Figure 15: The wind rose in wind farm of Ulyanovsk oblast of RF.

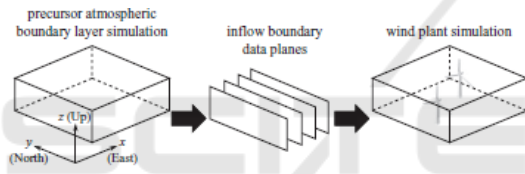Figure 16: The Weibull distribution and average velocity in wind farm of Ulyanovsk oblast of RF.

Figure 17: The procedure of "Precursor" method.

3.2 Results of Simulation

The flow patterns around four turbines aligned to the first row of the array were studied to determine the general behaviour of the resulting flow in the model wind farm. It was noted that the wakes behind the first turbines row are more stable, but with the second and the third turbine's rows the wake turbulent behaviour becomes more pronounced (Figure 18).
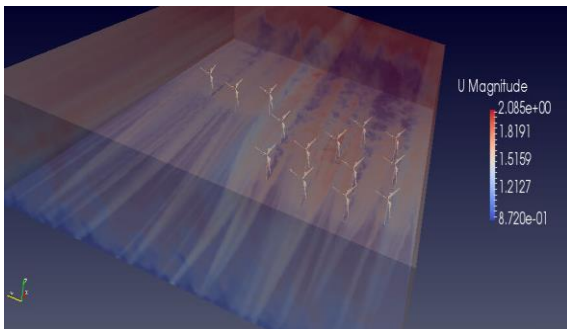

Figure 18: The numerical domain for wind farm simulation with 14 model wind turbines.

In order to study the value of the Energy Spectrum of turbulence E(k) with FFTW library a 3D box comprising an even mesh was created (Figure 19).
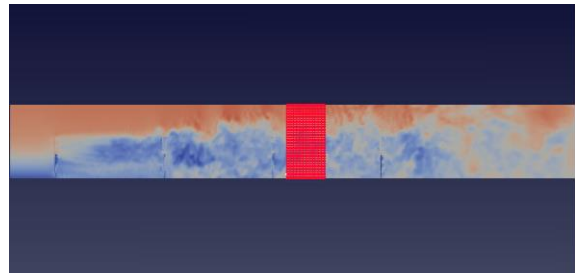

Figure 19: 3D box in numerical domain for calculation E(k).

The velocity field was then interpolated into the box and FFTW 3.3.8 library was applied. The calculated Energy Spectrum E(k) in Fourier space was closed to Kolmogorov-Obukhov k-5/3 spectrum and is shown on Figure 20 (Pope, 2000).

The calculations were carried out on the high performance computer cluster of ISPRAS in web-laboratory UNICFD using 12-72 computer cores for each numerical case.
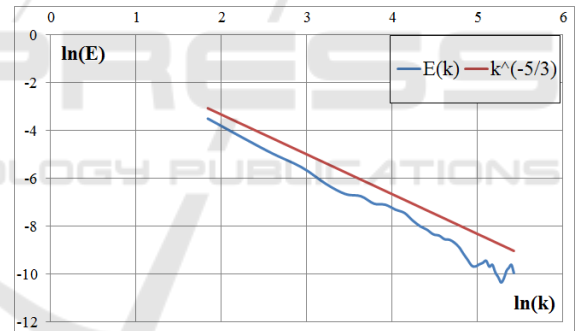

Figure 20: The Energy Spectrum E(k).

The simulation results for a model wind farm with 14 wind turbines for physical time t=1.0 second are presented in Table 1.

Table 1: The results of simulations.

Number of processors	Execution time (seconds)	Speedup
12 cores in 1 computer node	27650	-
36 cores in 3 computer nodes	9104	3.04
72 cores in 6 computer nodes	5842	4.73

4 CONCLUSIONS

We have used SOWFA library and ABLSolver solver to setup a case for ABL simulation with the complex mountain terrain for wind farm located in Crete near the village of Xirolimni. A LES simulation with a flat terrain using various solvers of SOWFA library was carried out for the Russian wind farm located in Ulyanovsk oblast RF. In connection with the small size of the wind turbines and the large velocity of blades rotation we can neglect some terms like the horizontal gradient of pressure and Coriolis force in momentum equation. This approach allows us to take into account the orography of the area, different physical processes in ABL like lower-level jets (Basu et al., 2010; Baas et al., 2009), large scale motions and vortices (Huang et al.,2009; Shah and Bou-Zeid, 2014), structure functions, scaling exponents and intermittency in turbulent wakes (Vindel, et al., 2008; Ali, et al., 2016). The method makes possible modelling of turbulent boundary layer flow over fractal-like multiscale terrain using LES (Yang and Meneveau, 2017) and assessing the impact of the wind farm and turbulent wakes on the local microclimate of the region.

ACKNOWLEDGEMENTS

REFERENCES

Mehta, D., et al. 2014. Large eddy simulation of wind farm aerodynamics: a review. *Journal of Wind Energy & Industrial Aerodynamics*, 133, pp.1–17.

Stevens, R.J.A.M., Meneveau, C., 2017. Flow Structure and Turbulence in Wind Farms. *Annual Review of Fluid Mechanics*, 49, pp. 311–39.

Tsoutsos, T., et al., 2015. Sustainable siting process in large wind farms case study in Crete. *Renewable Energy,* 75, pp. 474-480.

Kanellopoulos, D., et al., 2013. The Cretan wind farms. Estimating Energy Output in Areas of complex terrain. *Conference of the Wind Power Engineering Community.* Berlin, Germany, 18–19 June 2013.

Sagaut, P. 2002. *Large eddy simulation for incompressible flows: an introduction*, Berlin. Springer.

Germano, M., Piomelli, U., Moin, P., Cabot, W. H., 1991. A dynamic subgrid-scale eddy viscosity model. *Phys. Fluids*, 3, pp. 1760–1765.

Meneveau, C., Lund, T. S., Cabot, W. H., 1996. A Lagrangian dynamic subgrid-scale model of turbulence. *J Fluid. Mech*, 319, pp. 353–385.

Oliveira, P. J., Issa, R. I., 2001. An improved PISO algorithm for the computation of buoyancy-driven flows. *Numerical Heat Transfer*, 40 (B), pp. 473-493.

Schumann, U., 1975. Subgrid-Scale Model for Finite-Difference Simulations of Turbulent Flow in Plane Channels and Annuli. *Journal of Computational Physics,* 18, pp. 76–404.

Churchfield, M. J., Moriarty, P. J., Vijayakumar, G., Brasseur, J. G., 2010. Wind Energy-Related Atmospheric Boundary Layer Large-Eddy Simulation Using OpenFOAM. *19th Symposium on Boundary Layers and Turbulence*. Keystone, Colorado, USA, 2 - 6 August 2010. NREL.

Churchfield, M. J., Lee. S., Michalakes, J., Moriarty. P. J., 2012. A numerical study of the effects of atmospheric and wake turbulence on wind turbine dynamics. *Journal of Turbulence,* 13(14), pp. 1–32.

Tellez-Alvarez, J., Koshelev, K., Strijhak, S., Redondo, J.M., 2019. Simulation of turbulence mixing in atmosphere boundary layer and analysis of fractal dimension. *Physica Scripta,* [e-journal]. https://doi.org/10.1088/1402-4896/ab028c.

Kryuchkova, A., Tellez-Alvarez, J., Strijhak, S., Redondo J.M., 2017. Assessment of Turbulent Wake Behind Two Wind Turbines Using Multi-Fractal Analysis. *Ivannikov ISPRAS Open Conference (ISPRAS).* Moscow, Russia, 30 November – 1 December 2017. IEEE. https://doi.org/10.1109/ISPRAS.2017.00025

Strijhak, S.V., Koshelev, K.B., Kryuchkova, A.S., 2018. Studying parameters of turbulent wakes for model wind turbines. *AIP Conference Proceedings*, [e-journal] 2027, 030086 (2018). pp. 1-8. https://doi.org/10.1063/1.5065180.

Sørensen, J.N., Shen, W.Z., 2002. Numerical Modelling of Wind Turbine Wakes. *Journal of Fluids Engineering,* 124, pp.393-399.

Hancock P.E., Farr T.D., 2014. Wind-tunnel simulations of wind-turbine arrays on neutral and non-neutral winds. *J. Phys.: Conf. Ser.,* 524 012166.

Hancock, P.E., Pascheke, F., 2014. Wind-Tunnel Simulation of the Wake of a Large Wind Turbine in a Stable Boundary Layer: Part 2, the Wake Flow. *Boundary-Layer Meteorology,* 151, pp. 23–37.

Pierella, F., Krogstad, P.A., Sætran, L., 2014. Blind Test 2 calculations for two in-line model wind turbines where the downstream turbine operates at various rotational speeds. *Renewable Energy,* 70, pp. 62–77.

Pope S.B., 2000. *Turbulent Flows*, Cambridge. Cambridge University Press.

Basu, S. et al., 2010. Stable boundary layers with lower-level jets: what did we learn from the LES intercomparison within GABLS3? *The Fifth International Symposium on Computational Wind Engineering (CWE2010).* Chapel Hill, North Carolina, USA, 23-27 May 2010. pp. 1-8.

Baas, P., Bosveld, F.C., Klein Baltink, H., and Holtslag, A.A.M., 2009. A climatology of nocturnal low level jets

at Cabauw. *Journal of Applied Meteorology and Climatology*, 48, pp. 1627-1642.

Huang, J., Cassiani, M., Albertson, J. D., 2009. Analysis of coherent structures within the atmospheric boundary layer. *Boundary-Layer Meteorology,* 131, pp. 147–171.

Shah, S., Bou-Zeid, E., 2014. Very-Large-Scale Motions in the Atmospheric Boundary Layer Educed by Snapshot Proper Orthogonal Decomposition, *Boundary-Layer Meteorology*, 153 (3), pp. 355-387.

Vindel, J.M., Yage, C., Redondo, J.M., 2008. Structure function analysis and intermittency in the atmospheric boundary layer. *Nonlinear Processes Geophys.*, 15, pp. 915-929.

Ali, N., Aseyev, A.S., Cal R.B., 2016. Structure functions, scaling exponents and intermittency in the wake of a wind turbine array. *Journal of renewable and sustainable energy*, 8, pp. 013304-1 - 013304-9.

Yang, X.I.A., Meneveau, C. 2017. Modelling turbulent boundary layer flow over fractal-like multiscale terrain using large-eddy simulations and analytical tools. *Phil. Trans. R. Soc. A.*, 375, 20160098. pp.1-19. https://doi.org/10.1098/rsta.2016.0098.